Information System for Estimation Spatial Characteristics of Lineament Networks Derived from Satellite Images

Volodymyr Hnatushenko[a], Olga Korobko[a], Vasyl Lytvyn[b], Sergey Nikulin[a] and Kateryna Sergieieva[a]

[a] *Dnipro University of Technology, 19 av. Dmytra Yavornytskoho, Dnipro, 49005, Ukraine*
[b] *Lviv Polytechnic National University, 12 Bandera street, Lviv, 79013, Ukraine*

Abstract

Computer processing and analysis of satellite images are key stages in solving many problems of modern geology. Important objects of study are straight-line elements of images corresponding to natural linear features of the landscape – riverbeds, mountain ranges, vegetation boundaries, elongated chains of lakes or swamps, etc. Such elements are called lineaments and correspond to deep-seated rectilinear geological structures. Lineaments form networks that include several systems of fixed azimuths characteristic for the entire surface of the Earth. Analysis of lineaments and their spatial networks helps to investigate the deep structure of territories and solve various geological problems, including forecasting mineral resources and assessing seismic hazards. For this purpose, an information system was developed. It is aimed at estimating spatial characteristics of linear element networks derived from satellite images. The system allows evaluating various mathematical transformants of the original lineaments and their networks, generating ensembles of characteristics, each of which represents certain aspects of the spatial distribution of lineaments. The lineaments can be used directly to solve certain problems, as well as serve as initial data for various methods of data analysis, for example, reference classification, clustering, etc.

The article describes the specifics of natural lineament representation on satellite images, as well as approaches to their extraction. The description of 4 groups of spatial characteristics calculated using the developed information system, is given. The practical result of their use in solving the problem of gold ore forecasting on the territory of Uzbekistan is described, which demonstrates the high potential of the developed system. The system allows identifying large linear elements that are not directly distinguished in the images.

Keywords

Information system, satellite images, lineament, spatial analysis, GIS RAPID

1. Introduction

Lineament analysis of satellite images is an important area of modern geological research. It includes extraction, processing, and subsequent investigating of linear structures of natural origin, the so-called lineaments. Satellite image lineaments are their rectilinear fragments (Fig.1), corresponding to linear deep inhomogeneities of the Earth's crust, to which linear fragments correspond on the surface: a) hydrographic network, b) geological boundaries observable on the surface, c) vegetation boundaries of different types, and d) chains of small polygonal objects (such as lakes, etc.).

At the present time, there is a stable conception of the lineaments relationship with systems of various orders deep and near-surface faults, lines of maximum geodynamic activity, force lines of

IntelITSIS'2022: 3rd International Workshop on Intelligent Information Technologies and Systems of Information Security, March 23–25 2022, Khmelnytskyi, Ukraine
EMAIL: vvgnat@ukr.net (V. Hnatushenko); korobko.o.v@nmu.one (O. Korobko); vasyl17.lytvyn@gmail.com (V. Lytvyn); nikulin.s.l@nmu.one (S. Nikulin); sergieieva.k.l@nmu.one (K. Sergieieva)
ORCID: 0000-0003-3140-3788 (V. Hnatushenko); 0000-0002-7491-9162 (O. Korobko); 0000-0002-9676-0180 (V. Lytvyn); 0000-0003-1795-3599 (S. Nikulin); 0000-0001-7345-2209 (K. Sergieieva)

tectonic stress fields, as well as zones of increased permeability of the Earth's crust, etc. [1]. Lineaments may correspond to flumes of various solutes, zones of intense fluid dynamics, linear areas of improved reservoir fluid properties and, thus, can be used as direct indicators in the forecast and prospecting of mineral deposits. This substantiates the relevance and usefulness of lineament analysis.

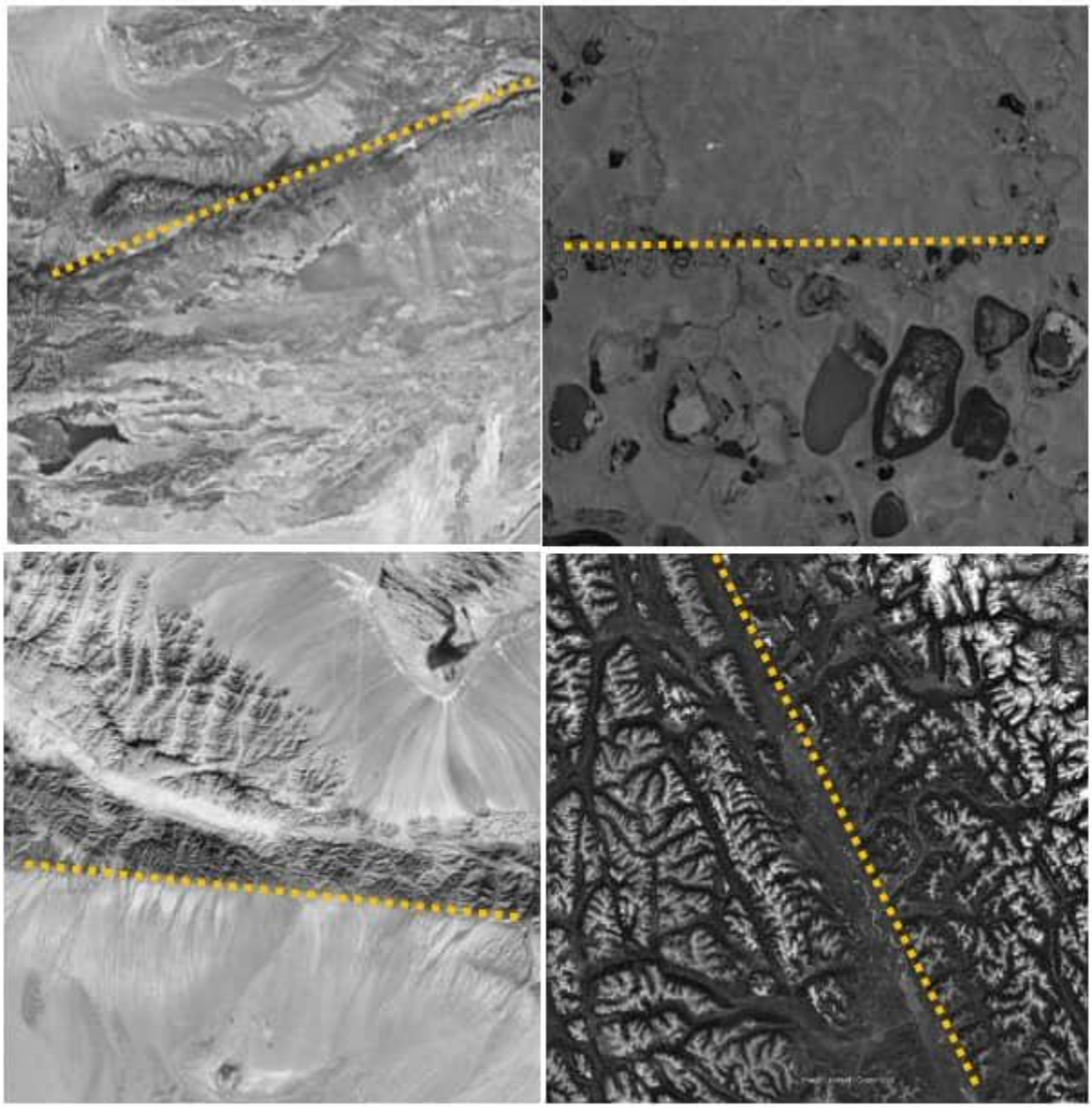

Figure 1: Examples of natural lineaments in satellite images

A peculiarity of such lineaments is their grouping into systems of certain fixed directions. The location of lineaments on the earth's surface is not random but obeys certain rules. Many researchers emphasize the presence of several basic fixed azimuths of lineaments orientation. Usually, there are 4 azimuths – 0, 45, 90, 135° [2-5]; azimuths of 30, 60, 120, and 150° are less common. Some researchers, for example, in [6-8], distinguish other azimuths of lineament systems orientation, not denying the dominant role of lineaments of sublatitudinal, submeridional, and two diagonal systems. The numerous authors' studies on lineament orientation in different parts of the Earth also confirm their dominant role [9].

There is a global network of lineaments, which significantly controls the localization of mineral deposits [10, 11]. A high percentage of known deposits are located within 1-5 km from regional linear elements [12].

These factors lead to the exceptional importance of improving the lineaments extraction and analysis quality as an important stage in solving predictive and prospecting geological problems.

2. Related Works

At present, the idea of automatic lineament detection and their statistical, morphometric, and spatial analysis is practically implemented in several ways.

Firstly, specialized algorithms and information systems are being developed, designed either only for automatic lineament extraction with their subsequent visual analysis, or for also providing some analysis opportunities, including the calculation of spatial statistical characteristics (density of lineaments, estimates of their orientation, etc.) [13, 14]. Some of the software is completely original developments, and some are modules created using the API of well-known systems, such as ArcGIS or Matlab.

Most lineament researchers take analyze lineaments in a different way based on customizing the individual tools of advanced and popular geoinformation systems (GIS) and geological information processing systems [15]. The most frequently used systems are ArcGIS, ERDAS Imagine, PCI Geomatica, ENVI, GeoRose, RockWorks, etc. [16]. Although these systems are not usually developed for lineament analysis, they contain a number of tools that can be successfully used, for example, for statistical analysis of linear objects and study of their spatial distribution. Often a combination of systems is used. In this case, their integration is provided at the level of data formats import-export, which complicates the analysis process, but provides a wider range of available tools.

The described approaches have their advantages and disadvantages. The advantages of specialized systems and modules are their focus on solving the problems of lineament analysis and a simpler interface, which provides the user with ease of operation and speed of development. The most important drawback is the limited toolkit, which does not allow solving related tasks and necessitates involving additional software.

The benefits and advantages of the approach based on the use of non-specialized systems are directly opposite. The complexity of their development and application is compensated by the ease of use of intermediate and final results in other modules when solving related problems [17].

The mentioned shortcomings were the reason for the creation of the information system described in this paper, which combines the advantages of these approaches with an attempt to minimize their shortcomings.

3. Proposed Methodology

3.1 Lineament Systems Extraction

Lineaments corresponding to linear natural formations have several features distinguishing them from linear objects of anthropogenic origin (such as roads, agricultural field boundaries, etc.). Natural formations, in addition to the fact that they often do not have clear boundaries (such as swamps), are repeatedly disturbed by horizontal tectonic movements. As a result, they are usually fragmented, ripped, and rotated relative to their initial position. This significantly complicates their extraction, so the known automatic methods of linear contours extraction (recognition) become ineffective or insufficient.

Currently, automatic extraction of lineaments (hereinafter – ALE) and their systems is performed in two stages: 1) generation of a binary contour map (by some mask algorithm, for example, the optimal Canny edge detector [18]), which corresponds to the boundaries of a sharp change in image brightness and 2) their subsequent processing for vector linear objects extraction. The second stage can be implemented as an object vectorization procedure and is usually performed based on the Hough transform and its various modifications. The Hough transform allows extraction of straight lines on a contour image with a predefined accuracy [19].

The idea of the Hough transform is to find curves going through a sufficient number of points of interest (i.e., single pixels on brightness boundary maps). The set of curves on a plane, determined by the parametric equation, looks as follows:

$$F(a_1, a_2, \dots, a_n, x, y) = 0, \quad (1)$$

where F – some function; $a_1, a_2, \ldots, a_n$ – parameters of a set of curves; x, y – coordinates on a plane.

The parameters of a set of curves form a phase space, each point of which (specific values of the parameters $a_1, a_2, \ldots, a_n$) corresponds to a certain curve. Due to the discreteness of digital images, it is required to convert the continuous phase space into a discrete one. For this, a network is introduced in the phase space, dividing it into cells, each of which corresponds to a set of curves with close parameter values. Each cell of the phase space can be associated with a counter indicating the number of points of interest in the image that belong to at least one of the curves corresponding to this cell. The analysis of the cell counters allows to find the curves with the largest number of points of interest. There are many modifications and varieties of Hough transforms that usually give better results than the basic Hough transform.

To date, many computer methods and information technologies of lineament automatic extraction have been created [4, 20-22]. However, despite the developed mathematical and software tools for the automated extraction of brightness boundaries and lineaments based on the Canny detector and the Hough transform, their use in geology has some fundamental difficulties indicated above. Therefore, the so-called "interactive" extraction of lineaments (IEL) is performed by an expert decoder manually from the analyzed image. The final decision on extracting or not extracting the lineament is made by an expert [23].

Both approaches have their advantages and disadvantages. The declared advantages of ALE are rapidity and simplicity of operation, as well as the objectivity of the results obtained. At the same time, the main disadvantages that are traditionally attributed to IEL are subjectivity and the requirement for the high qualifications of a decoder (preferably, several decoders) to obtain reliable results. However, in practice, the automatic approach is subjective to some degree: a specialist can influence the results of lineaments extraction through the choice of software, a specific algorithm, methods of image preprocessing, various parameters, and threshold values.

Therefore, automatic extraction should necessarily be supported by an interactive one using GIS tools, the knowledge and experience of a geologist-decoder, and the colossal recognition capabilities of the human brain when working with 2D images.

3.2 Calculation of Lineament Network Characteristics

The most important stage of lineament analysis is estimation of spatial characteristics of the previously extracted lineaments and their systems. Characteristics are evaluated using a variety of mathematical functions that transform vector or binary lineament maps into raster grids, where each cell is assigned some integer or real value. The obtained characteristics can be both of independent importance in solving forecast problems or can be used in further calculations as input data.

In this regard, a subsystem for estimation the lineament networks characteristics was developed as a part of the geoinformation system RAPID, developed by specialists of the Dnipro University of Technology [24, 25].

The GIS RAPID is focused on processing and intelligent analysis of heterogeneous and multi-level geodata, and allows, on general methodological principles, to solve a wide range of the Earth sciences issues – mineral deposits forecasting, territories regionalization, monitoring, and forecasting of various geoecological situations, etc.

The system includes data management core, and a set of about 100 modules grouped into functional subsystems with a single user interface. The system core is a software package consisting of two components. The first is responsible for calling individual modules, for data exchange between different modules (that solve specific tasks of data processing and analysis), as well as between GIS RAPID and such well-known systems as ArcGIS, Micromine, Surfer, and others. The second is embedded in all functional modules, manages data streams, and provides reading, writing, deleting, visualizing tools and simple transformations (smoothing, filling gaps, normalization) [25].

The GIS RAPID technology is based on the methods of Data Mining, image processing [24], mathematical statistics, lineament, and spatial geoinformation analysis [25]. It implements the principle of multivariate problem solving using simulation and computational experiments.

Four subtypes of lineament network characteristics are implemented. All of them are calculated using the sliding vicinity (window) principle when the pixels values falling inside a rectangular or elliptical region of a fixed size are used for calculations, and the result is assigned to the central pixel of a window. A sliding vicinity

moves across the image in such a way that its center consistently coincides with all the pixels of the image (except for the edge ones, so-called "borders").

The ***first subtype*** of characteristics is based on all the extracted lineaments and provides information about:

- the density of lineaments (the number of lineaments in the vicinity divided by its area);
- the total length of lineaments inside a vicinity (total length of lineaments inside a window, divided by its area);
- the average length of lineaments within a vicinity;
- the density of lineaments intersection nodes (the number of lineaments intersections divided by the vicinity area);
- the number of lineament directions in a vicinity;
- the prevailing azimuth of the lineaments, etc.

The ***second subtype*** transformations are based on calculating the characteristics of the lineaments of individual fixed azimuths. As mentioned earlier, there are two main systems of lineaments with azimuths 0-90º and 45-135º. In some areas, there are also other systems, for example, with azimuths of 30-120º or 60-150º. Based on the rose diagram analysis of lineament distribution in the study area, it is possible to determine the number and azimuths of lineaments prevailing directions and, using a sliding vicinity, calculate their characteristics, in particular, density, in a network cells.

Transformations of the ***third subtype*** are based on the calculation of various ratios between the densities of differently oriented lineaments. If there are 4 main directions with azimuths 0, 45, 90, and 135º, the following characteristics can be evaluated:

$$L_1=\frac{N_0+N_{90}}{N_{45}+N_{135}}, \tag{2}$$

$$L2=|N_0-N_{90}|+|N_{45}+N_{135}|, \tag{3}$$

$$L3=\frac{N_0+N_{90}}{N_0+N_{90}+N_{45}+N_{135}}, \tag{4}$$

$$L4=\frac{N_0}{N_0+N_{45}+N_{90}+N_{135}}, \tag{5}$$

$$L5=\frac{N_{90}}{N_{90}+N_{90}+N_{90}+N_{135}}, \tag{6}$$

$$L6=\frac{N_0}{N_{45}+N_{90}+N_{135}}, \tag{7}$$

$$L7=\frac{N_{90}}{N_0+N_{45}+N_{135}}, \tag{8}$$

$$L8=D(N_0,N_{90},N_{45},N_{135}), \tag{9}$$

$$L9=\max(N_0,N_{90},N_{45},N_{135}), \tag{10}$$

$$L10=\min(N_0,N_{90},N_{45},N_{135}), \tag{11}$$

$$L11=L_{10}-\frac{N_0+N_{90}+N_{45}+N_{135}}{4}, \tag{12}$$

$$L12=\begin{cases}1 & if\ L_{10}=N_0\\ 2 & if\ L_{10}=N_{45}\\ 3 & if\ L_{10}=N_{90}\\ 4 & if\ L_{10}=N_{135}\end{cases},\quad L13=\begin{cases}1 & if\ L_{11}=N_0\\ 2 & if\ L_{11}=N_{45}\\ 3 & if\ L_{11}=N_{90}\\ 4 & if\ L_{11}=N_{135}\end{cases} \tag{13}$$

where N_0, N_{90}, N_{45}, N_{135} – density of lineaments with azimuths, respectively, *0±22.5°*, *45±22.5°*, *90±22.5°*, and *135±22.5°* in a cell vicinity; D – variance calculated from N_0, N_{90}, N_{45}, N_{135}.

The obtained characteristics $L_1 – L_8$ and L_{11} are different measures of fracture anisotropy, and L_2 describes the distortion of a lineament network. The L_3-L_7 characteristics are less dependent on factors

that impede lineament extraction in automatic mode (such as cloud cover or overlying Quaternary deposits), since they represent a quotient of quantities equally susceptible to interfering factors.

Characteristics L_9 and L_{12} describe the predominant direction of fracturing at each point of the network (their density and azimuth, respectively), L_{10} and L_{13} – on the contrary, the rarest direction of lineaments.

Several other fracture characteristics have also been proposed, for example:

$$L_{14} = K/N, \tag{14}$$

where N – the total density of lineaments in a sliding window; K – the number of lineaments directions in the vicinity.

The L_{14} characteristic, along with K, is a kind of measure of geological structure complexity, but, unlike K, it lesser depends on the presence or absence of interfering factors decreasing the total density of lineaments identified.

$$L_{15} = \frac{N_{90}}{N_0+N_{90}}; \quad L_{16} = \frac{N_0}{N_0+N_{90}}, \tag{15}$$

$$L17 = \begin{cases} 1 & if \quad N_0 > N_{90} \\ 0 & if \quad N_0 \le N_{90} \end{cases} \tag{16}$$

These characteristics describe the state of a lineament network consisting of mutually perpendicular elements with azimuths of $0°$ and $90°$.

The following characteristics are also of interest:

$$L_{18} = \left(N_0^2 + N_{90}^2 + N_{90}^2 + N_{135}^2\right) - (N_0 + N_{45} + N_{90} + N_{135})^2, \tag{17}$$

$$L19 = 0.25[(N_0 \cos(0) + N_{45} \cos(45) + N_{90} \cos(90) + N_{135} \cos(135))^2 + (N_0 \sin(0) + N_{45} \sin(45) + N_{90} \sin(90) + N_{135} \sin(135))^2]^{0.5} \tag{18}$$

In some parts of the Earth's crust, in addition to the main lineament strike azimuths, several additional ones are also distinguished. If there is a third system of lineaments on the site with azimuths, for example, $30\text{-}120°$, the following characteristics can be evaluated:

$$L'_1 = \frac{N_0+N_{90}}{N_{30}+N_{120}+N_{45}+N_{135}}; \; L'_2 = \frac{N_{30}+N_{120}}{N_0+N_{90}+N_{45}+N_{135}}; \; L'_3 = \frac{N_{45}+N_{135}}{N_0+N_{90}+N_{30}+N_{120}}; \tag{19}$$

$$L'4 = |N_0 - N_{90}| + |N_{30} - N_{120}| + |N_{45} - N_{135}|; \tag{20}$$

$$L'5 = |N_0 - N_{90}| + |(N_{45} + N_{135}) - (N_{30} + N_{120})|; \tag{21}$$

$$L'6 = |(N_0 + N_{90}) - (N_{30} + N_{120})| + |(N_0 + N_{90}) - (N_{45} + N_{135})| + |(N_{30} + N_{120}) - (N_{45} + N_{135})|; \tag{22}$$

$$L'7 = D(N_0, N_{30}, N_{45}, N_{90}, N_{120}, N_{135}); \tag{23}$$

$$L'8 = max(N_0, N_{30}, N_{45}, N_{90}, N_{120}, N_{135}); \tag{24}$$

$$L'9 = min(N_0, N_{30}, N_{45}, N_{90}, N_{120}, N_{135}); \tag{25}$$

$$L'10 = L_8 - \frac{1}{6}(N_0 + N_{30} + N_{45} + N_{90} + N_{120} + N_{135}); \tag{26}$$

$$L'11 = K/N; \tag{27}$$

$$L'12 = \left(N_0^2 + N_{30}^2 + N_{45}^2 + N_{90}^2 + N_{120}^2 + N_{135}^2\right) - (N_0 + N_{30} + N_{45} + \\ + N_{90} + N_{120} + N_{135})^2, \quad (28)$$

where N_0, N_{30}, N_{45}, N_{90}, N_{120}, N_{135} – density of lineaments with azimuths, respectively, $0\pm\varepsilon°$, $30\pm\varepsilon°$, $45\pm\varepsilon°$, $90\pm\varepsilon°$, $120\pm\varepsilon°$ i $135\pm\varepsilon°$ in the vicinity of the network cell; ε – permissible angle of lineaments deviation from prevailing azimuths; N – total density of lineaments in a cell vicinity; K – number of lineament directions within the vicinity; D – variance estimate calculated for values N_0, N_{30}, N_{45}, N_{90}, N_{120}, N_{135}.

For the case of 8 main lineament azimuths, similar characteristics are evaluated.

The main purpose of all the characteristics described above is categorization territory depending on lineament network properties and, presumably, the nature of fracturing, as well as the identification boundaries of such zones in order to clarify the geological structure and tectonic setting.

The characteristics of lineament networks of the ***fourth subtype*** are formed based on an analysis of their rose diagrams in a sliding vicinity. The rose diagram represents the lineaments orientation in a vicinity (Fig. 2). The set of rose diagrams forms the so-called field of rose diagrams being further processed.

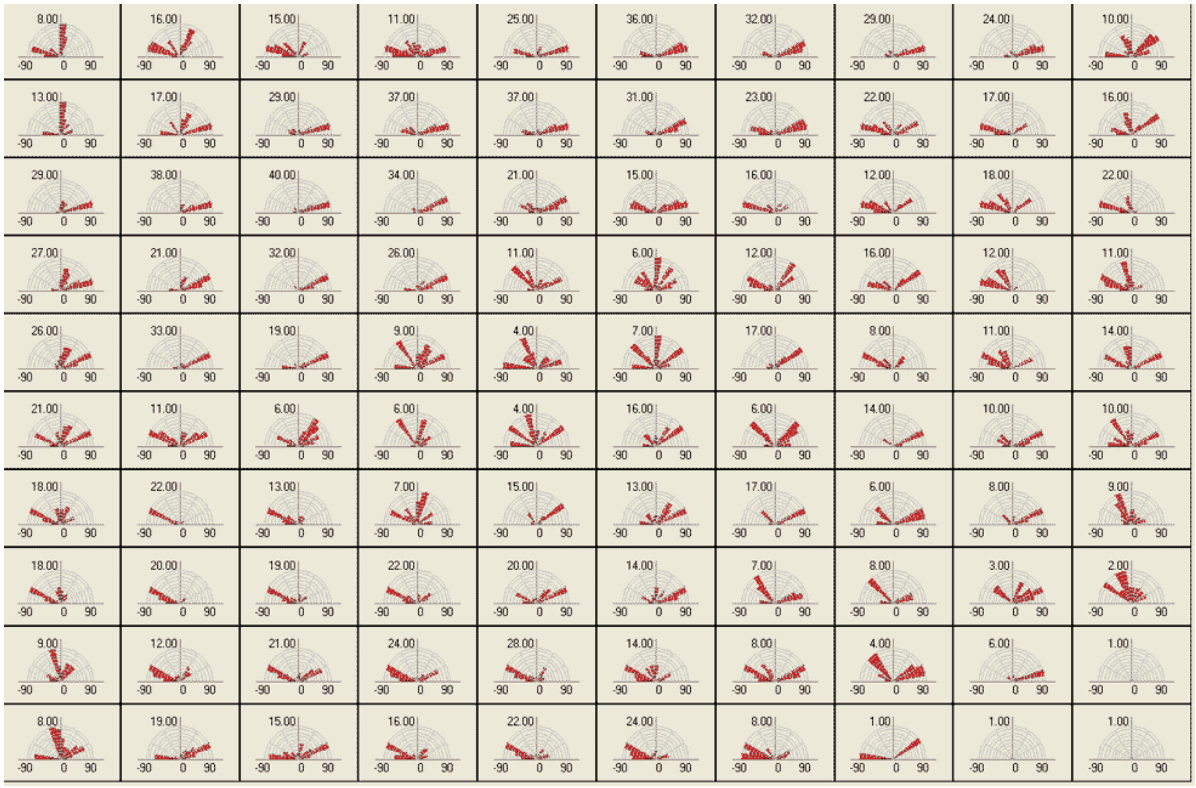

Figure 2: An example of a field of rose diagrams, generated from the extracted lineaments in an image space

The system allows the calculation of several characteristics, including the similarity of rose-diagram with a cross, the azimuth of prevailing main direction, the rose elongation, its proximity to the circle, and several others.

4. Results and Discussions

The developed subsystem of lineament analysis was tested in solving several practical problems [9]. Below are some practical examples of its work on the territory of the Jamansai Mountains (Uzbekistan, Fig. 3). This site is located in a mid-mountainous area and contains a number of points with high gold content. Multiband imagery from the QuickBird 2 satellite was used. The spatial resolution of

panchromatic images is 0.6 m, multispectral (4 bands – red, green, blue, and near infrared) – 2.5 m. Previously, the panchromatic and multispectral bands were combined using the ERDAS Imagine 8.7 software, which allowed to obtain multispectral images with a resolution of up to 0.6 m for further processing. This resolution roughly corresponds to a scale of 1:5000.

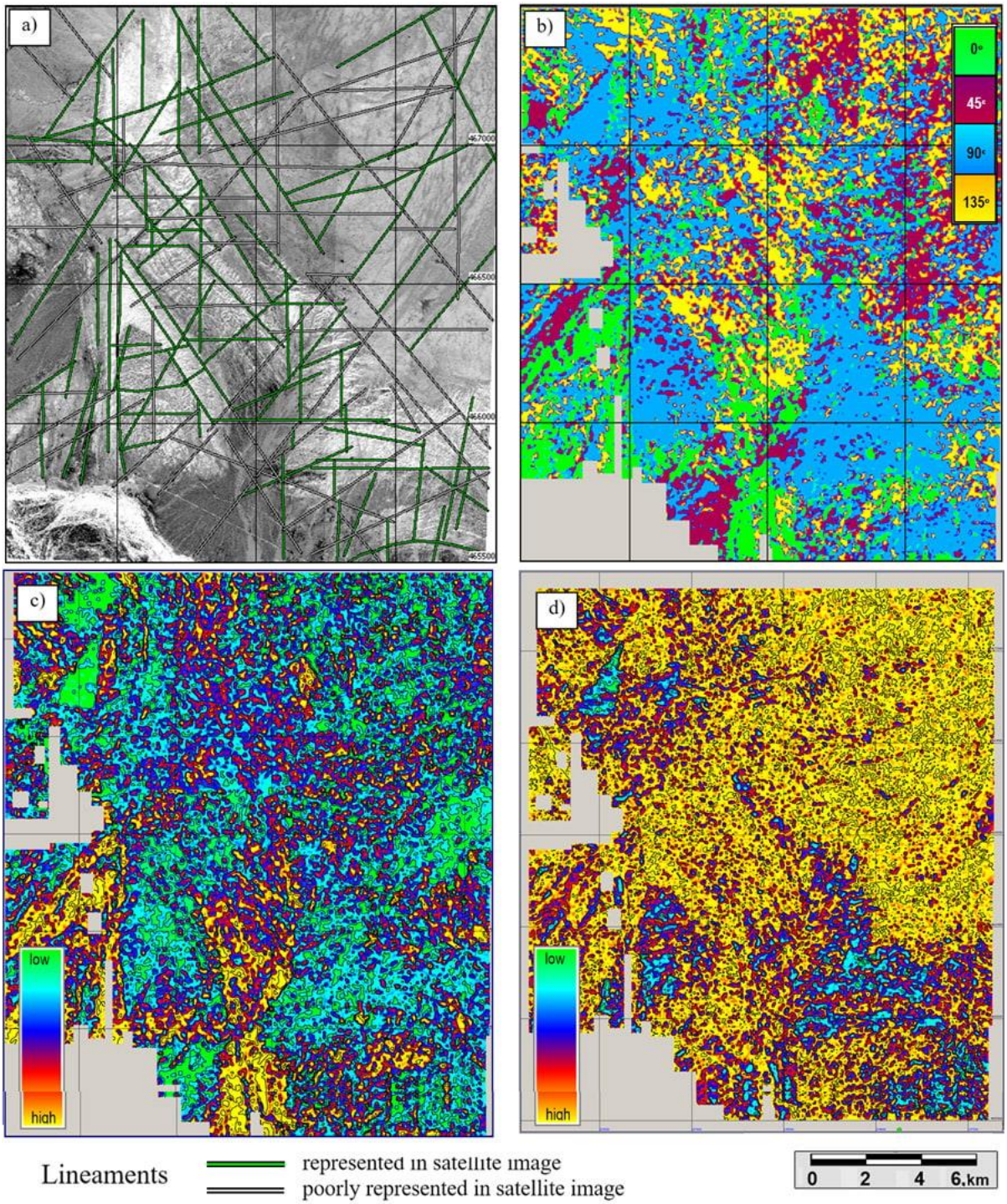

Figure 3: a) satellite image of a site of Jamansai Mountains (Uzbekistan); b) map of L_{10} (predominant direction of lineaments); c) map of L_4 (the ratio of lineaments density with azimuth 0±22.5° to the total density of lineaments); d) map of L_{11} (difference of L_{10} and average density of lineaments)

Several large linear structures were identified in the automatic mode; the lineament network has been improved interactively. It should be noted that several objects visually indistinguishable in the

original image were extracted (gray lines in Fig. 3a). In Fig. 3a, for the simplicity of perception, the most extended lineaments are represented.

Fig. 3b-d show some of the calculated characteristics. They were used as input data for reference classification; points with a high gold content were used as the reference objects. The result is shown in Fig. 4. As it can be seen, most of these points fall into zones of increased prospect, which allows to consider such zones as promising for gold ore mineralization.

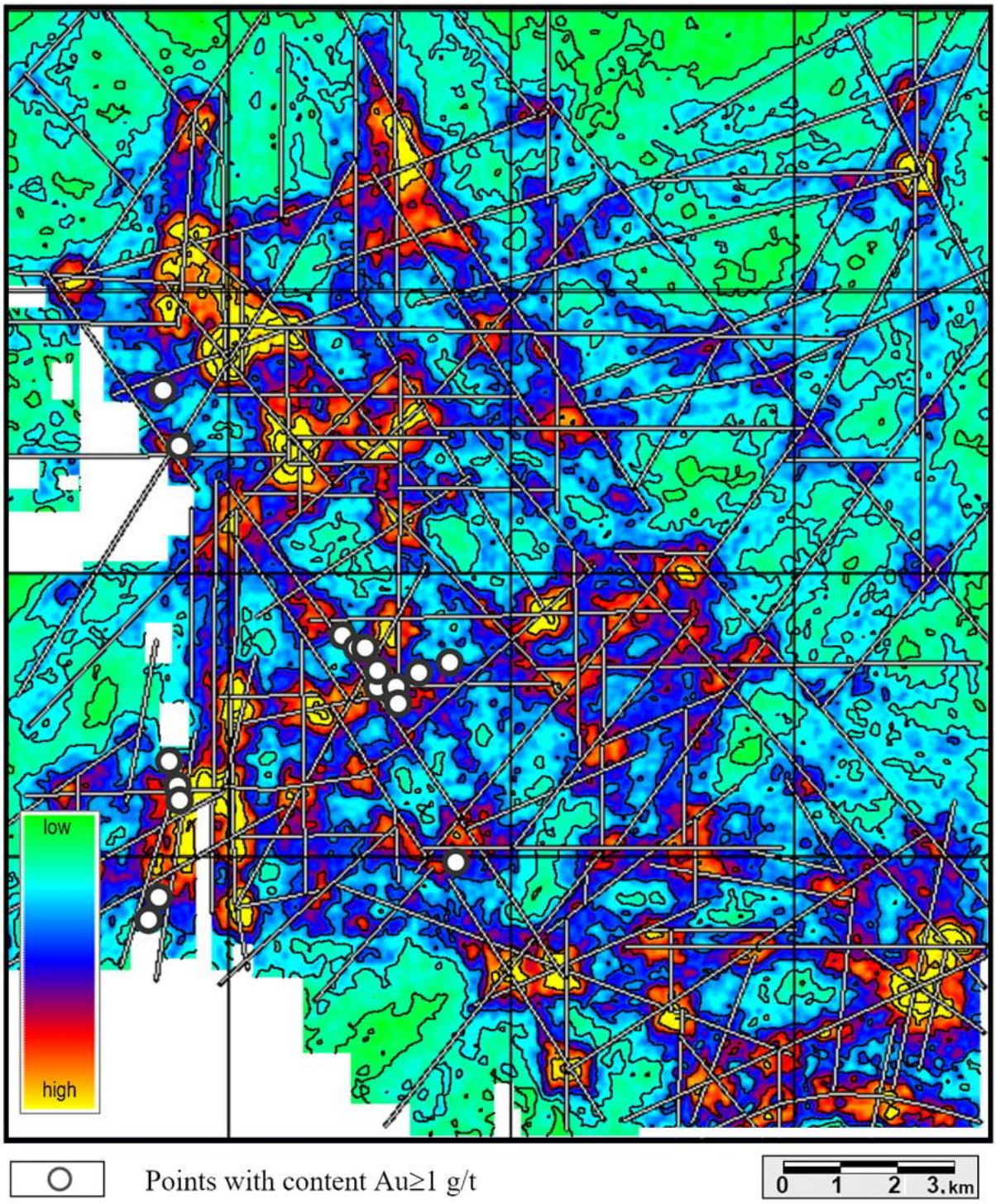

Figure 4: Map of the territory's prospects for the detection of gold ore mineralization (conventional units); generated based on lineament networks characteristics classification from satellite image

5. Conclusions

The authors have developed an information system for natural lineaments extraction and processing from satellite images. The system allows extracting additional geological information from the original images, which cannot be extracted by traditional methods of satellite imagery analysis. The analysis of the obtained results allows, among other things, to identify deep structural elements that are not directly identifiable on the images, which significantly increases their information content when solving geological problems.

The implemented subsystem for calculating spatial characteristics of lineaments and their networks makes it possible to obtain raster maps, which can later be used in various computational procedures, including reference classification as well as to generate maps representing the prospects of the territory for the discovery of mineral deposits and other geological objects. Such subsystems are either not implementer in the known software packages for space information processing, or are represented only by lineaments extraction modules, without their in-depth analysis.

The system is easily expandable by adding new methods for lineaments extraction and their spatial transformation. Currently, the tools for matching the results obtained by processing individual image bands are not implemented, which is a disadvantage, but also a promising direction in subsystem development. Moreover, additional opportunities may open when using ensembles of images of different spatial resolution, which will not only increase the reliability of identifying hidden structural elements of the geological environment but also provide information about their distribution in depth.

6. References

[1] Z. Liu, L. Han, C. Du, H. Cao, J. Guo, H. Wang. Fractal and Multifractal Characteristics of Lineaments in the Qianhe Graben and Its Tectonic Significance Using Remote Sensing Images. Remote Sensing, Vol. 13(4), 2021, p. 587. doi:10.3390/rs13040587.

[2] S. Essaa Khalid, G. Nadyb Abdelmohsen, S.Mostafa Mohamed, Elhussein Mahmoud. Implementation of potential field data to depict the structural lineaments of the Sinai Peninsula, Egypt. Journal of African Earth Sciences, Vol. 147, 2018, pp. 43-53. doi:10.1016/j.jafrearsci.2018.06.013.

[3] T. Zhang, S. Fan, S. Chen, S. Li, Y. Lu. Geomorphic evolution and neotectonics of the Qianhe River Basin on the southwest margin of the Ordos Block, North China. Journal of Asian Earth Sciences, Vol. 176, 2019, pp. 184–195. doi:10.1016/j.jseaes.2019.02.020.

[4] M.A. Enoh, F.I. Okeke, U.C. Okeke. Automatic lineaments mapping and extraction in relationship to natural hydrocarbon seepage in Ugwueme, South-Eastern Nigeria. Geodesy and Cartography, Vol. 47(1), 2021, pp. 34-44. doi:10.3846/gac.2021.12099.

[5] A. Javhar, X. Chen, A. Bao, A. Jamshed, M. Yunus, A. Jovid, T. Latipa. Comparison of multi-resolution optical Landsat-8, Sentinel-2 and radar Sentinel-1 data for automatic lineament extraction: A case study of Alichur area, SE Pamir. Remote Sensing, Vol. 11(7), 2019, p. 778. doi:10.3390/rs11070778.

[6] N. Raj, A. Prabhakaran, A. Muthukrishnan. Extraction and analysis of geological lineaments of Kolli hills, Tamil Nadu: a study using remote sensing and GIS. Arabian Journal of Geosciences, Vol. 10, 2017, p. 195. doi:10.1007/s12517-017-2966-4.

[7] K. Nedjraoui, M. Hamoudi, R. B. E. Khaznadji, S. Oughou, A. Bendaoud. Structural mapping and interpretation of lineaments related to the In Teria volcanism (southeastern Algeria) using Landsat 8 OLI TIRS images and aeromagnetic data. Journal of African Earth Sciences, Vol. 184, 2021, p. 104348. doi:10.1016/j.jafrearsci.2021.104348.

[8] V.V. Pokalyuk, I.E. Lomakin, V.G. Verkhovtsev, V.V. Kochelab. A framework of tectonic lineaments of the Black Sea region and surrounding areas of the Mediterranean Mobile Belt. Geoinformatics – European Association of Geoscientists & Engineers, Conference Proceedings, Geoinformatics, May 2021, pp. 1-6. doi:10.3997/2214-4609.20215521038.

[9] S.L. Nikulin, K.L. Sergieieva, O.V. Korobko. Computer detection of the Earth's crust blocks using satellite image lineaments. Conference Proceedings, Geoinformatics: Theoretical and Applied Aspects, May 2020, pp. 1-5. doi:10.3997/2214-4609.2020geo109.

[10] P.L. Keshava Kiran Kumar, G. Veeraswamy Yadav, K. Raghubabu, E. Balaji. Geochemical characteristics of iron ore deposits and processing of Landsat-8 data (geology, geomorphology and lineaments) in semi-arid region and using geospatial techniques. Modeling Earth Systems and Environment, Vol. 6(2), 2020, pp. 1245-1252. doi:10.1007/s40808-020-00754-5.
[11] S. Ysbaa, O. Haddouche, A. Boutaleb, M. Chemam, M. Sadaoui. Mineral deposits of northeastern Algeria (southern Medjerda mounts and diapiric zone): regional-scale structural controls, spatial distribution, and importance of geophysical lineaments. Arabian Journal of Geosciences, Vol. 12(15), 2019, pp. 1-13. doi:10.1007/s12517-019-4611-x.
[12] C. Ouko, F. Mutua, M. Mwaniki. A pre-exploration technique for mapping petroleum potential areas based on induced surface alterations and possible traps. Universal Journal of Geoscience, Vol. 6(5), 2018, pp. 158-174. doi:10.13189/ujg.2018.060503.
[13] L. Han, Z. Liu, Y. Ninga, Z. Zhaoa. Extraction and analysis of geological lineaments combining a DEM and remote sensing images from the northern Baoji loess area. Advances in Space Research, Vol. 62(9), 2018, pp. 2480-2493. doi:10.1016/j.asr.2018.07.030.
[14] Haeruddin, and J.F. Irawan. Identifying of the relationship between lineament density and vegetation index at Tumpangpitu Mining Area, East Java, Indonesia. AIP Conference Proceedings, Vol. 2278, No. 1, 2020, p. 020006. doi:10.1063/5.0014701.
[15] H. Ahmadi, and E. Pekkan. Fault-Based Geological Lineaments Extraction Using Remote Sensing and GIS – A Review. Geosciences, Vol. 11, no. 5, 2021, p. 183. doi:10.3390/geosciences11050183.
[16] S. Ghosh, T. Sivasankar, G. Anand. Performance evaluation of multi-parametric synthetic aperture radar data for geological lineament extraction. International Journal of Remote Sensing, Vol. 42(7), 2021, pp. 2574-2593. doi:10.1080/01431161.2020.1856963.
[17] A. Masoud, and K. Katsuaki. Applicability of computer-aided comprehensive tool (LINDA: LINeament Detection and Analysis) and shaded digital elevation model for characterizing and interpreting morphotectonic features from lineaments. Computers & Geosciences, Vol. 106, 2017, pp. 89-100. doi: 10.1016/j.cageo.2017.06.006.
[18] M. Mohammadpour, A. Bahroudi, M. Abedi. Automatic Lineament Extraction Method in Mineral Exploration Using CANNY Algorithm and Hough Transform. Geotectonics, Vol. 54, Issue 3, 2020, pp. 366-382. doi:10.1134/S0016852120030085.
[19] H. Ahmadi, E. Pekkan. Fault-Based Geological Lineaments Extraction Using Remote Sensing and GIS – A Review. Geosciences, Vol. 11(5), 2021, p. 183. doi:10.3390/geosciences11050183.
[20] A. Farah, A. Algouti, A. Algouti, M. Errami, and M. Ifkirne. Lithological mapping and automatic lineament extraction using Aster and Gdem data in the Imini-Ounilla-Asfalou district, South High Atlas of Marrakech, Morocco. In E3S Web of Conferences, Vol. 240, 2021. doi:10.1051/e3sconf/202124004002
[21] E. Farahbakhsh, R. Chandra, H. Olierook, R. Scalzo, C. Clark and oth. Computer vision-based framework for extracting tectonic lineaments from optical remote sensing data / International Journal of Remote Sensing Vol. 4, Issue 5, 2020, pp. 1760-1787. doi:10.1080/01431161.2019.1674462.
[22] X. Junlong, W. Xingping, Z. Haonan, L. Dayou, L. Jinbo, X. Lianglong, Y. Min. Automatic extraction of lineaments based on wavelet edge detection and aided tracking by hillshade. Vol. 65, Issue 1, 2020, pp. 506-517. doi:10.1016/j.asr.2019.09.045
[23] H.S. Aldharab, S. Ali, J. Ikbal, S.A. Ghareb. Spatial Analysis of Lineaments and Their Tectonic Significance Using Landsat Imagery in Alarasah Area-Southeastern Central Yemen. Journal of Geography, Environment and Earth Science International, 2018, Vol. 18(2), pp. 1-13. doi:10.9734/JGEESI/2018/45638.
[24] V.J. Kashtan, V.V. Hnatushenko and Y.I. Shedlovska. Processing technology of multispectral remote sensing images. 2017 IEEE International Young Scientists Forum on Applied Physics and Engineering (YSF), 2017, pp. 355-358. doi:10.1109/YSF.2017.8126647.
[25] B.S. Busygin, S.L. Nikulin, K.L. Sergieieva. Solving the tasks of subsurface resources management based on the created GIS RAPID geoinformation technology. Mining of Mineral Deposits. Vol. 3(13), 2019, pp. 49-57. doi:10.33271/mining13.03.049.